

## Evaluation of nuclear excitation by electronic transition in $^{235}\text{U}$ plasma at local thermodynamic equilibrium

P. Morel, V. Méot, and G. Gosselin

*Commissariat à l'Energie Atomique, Service de Physique Nucléaire, Boîte Postale 12, 91680 Bruyères-le-Châtel, France*

D. Gogny and W. Younes

*Lawrence Livermore National Laboratory, Livermore, California 94551, USA*

(Received 24 November 2003; published 23 June 2004)

A complete calculation of the nuclear excitation by electronic transition (NEET) rate of the first excited state of  $^{235}\text{U}$  in a local thermodynamic equilibrium (LTE) plasma is presented. The microscopic dynamics of the NEET probability are described allowing a clear description of the coupling between the atomic and nuclear transitions for the NEET effect. The atomic properties are estimated in the framework of a relativistic average-atom model. The statistical nature of the electronic transition spectrum is described by the mean of a Gaussian distribution around the average-atom configuration. The analysis of characteristic times occurring in the NEET probability allows one to calculate an equivalent excitation rate in a LTE  $^{235}\text{U}$  plasma. In the density-temperature plane, the NEET rate is strongly structured, showing the most relevant hydrodynamic conditions for the NEET process. The number of  $^{235}\text{U}$  nuclei, excited up to the 76.8 eV isomeric level in a high-intensity laser shot, has also been estimated.

DOI: 10.1103/PhysRevA.69.063414

PACS number(s): 33.25.+k, 25.30.-c, 23.20.-g

### INTRODUCTION

Nuclear excitation by electronic transition (NEET) [1,2] designates a mechanism of nuclear excitation induced by a transition between two bound states of the atomic system. The mechanism is very similar in nature to the inverse internal conversion where an electron in the continuum is captured with a subsequent excitation of the nucleus. Experimental works on  $^{197}\text{Au}$  [3] and  $^{189}\text{Os}$  [4,5] reveal that the probability for a NEET event to occur is very small.

Theoretical considerations indicate that an optimization of the NEET process depends on two essential parameters. One of these is the so-called mismatch in energy, defined as the difference between the energy of the atomic and nuclear transitions. Clearly the mismatch has to be as small as possible in order to be close to a resonant coupling. The other parameter is related to the size of a matrix element characterizing the electromagnetic interaction between the initial and final states of the nucleus-atom system. A nonvanishing, large matrix element requires that the nuclear and electronic transitions share a common multipolarity, which must be as low as possible. In normal situations, where the electronic transition involves simple configurations of the isolated atom, these two conditions are generally not satisfied simultaneously with great accuracy. For instance, for the two nuclei of Refs. [3–5],  $^{197}\text{Au}$  (with mismatch  $\delta=74.18$  eV) and  $^{189}\text{Os}$  ( $\delta=1261.5$  eV), the theory [6] predicts small NEET probabilities of  $3.57 \times 10^{-8}$  and  $1.13 \times 10^{-10}$ , respectively. If the energies of the atomic and nuclear transitions had been perfectly matched, these probabilities would have been of the order of  $1.06 \times 10^{-7}$  and  $1.8 \times 10^{-7}$ , respectively. These results give a measure of the sensitivity of the NEET probability to the mismatch condition.

Theoretical arguments and a number of experimental studies [7–11] indicate that the coupling of the nucleus to the

atomic electron system depends crucially on the degree of ionization of the atom, and more generally on its environment. Hot dense plasmas offer the possibility to study the NEET process in various situations where the atoms are ionized and distributed over a great variety of electronic configurations. In this paper, we investigate the behavior of the NEET probability as a function of the temperature and density characterizing a  $^{235}\text{U}$  plasma at local thermodynamic equilibrium (LTE).

Such a plasma can be reached by using a high-power laser. Various attempts have been made to measure the excitation rate of  $^{235m}\text{U}$  (76.8 eV,  $J^\pi=1/2^+$ ,  $t_{1/2} \approx 26$  min) in a laser-generated plasma. The first attempt, due to Izawa *et al.* [12], used a plasma heated by a  $\text{CO}_2$  laser. The authors claimed they excited the first isomeric state. *et al.* [13] tried to reproduce the experiment unsuccessfully, even though they used a pure  $^{235}\text{U}$  sample. More recent experiments have used a Nd laser to heat the plasma [14,15], but were also unsuccessful in populating the isomer.

Harston and Chemin [16] have considered the different mechanisms that could be responsible for nuclear excitation in a plasma of the first isomeric state of  $^{235}\text{U}$ , namely, NEET, nuclear excitation by electron capture (NEEC) from the continuum, photoexcitation, and inelastic electron scattering. The authors in Ref. [16] calculated the NEET rate for isomer excitation and showed that  $6p_{1/2}-5d_{5/2}$  and  $6d_{5/2}-6p_{1/2}$  electronic transitions are resonant with the nuclear transition at, respectively, 20 eV and 100 eV. The lower temperature associated with the  $6p_{1/2}-5d_{5/2}$  transition leads to a lower NEET rate. Harston and Chemin concluded that the NEET rate of the  $6d_{5/2}-6p_{1/2}$  atomic transition can be maximized under plasma conditions. The main difficulty in such a calculation lies in developing a good description of the atomic properties and an accurate representation of the statistical nature of the electronic spectrum. In plasma, the atomic con-

figuration number may be very large. Taking into account this large number of configurations requires that approximations be made in the atomic description. In Ref. [16], the calculation was made in the multiconfiguration Dirac-Fock formalism with a limited number of configurations. A collisional-radiative model [17], describing the laser-induced plasma, was used to get the population density in different charge states. We present here a calculation of excitation rates under the hypothesis of LTE. Such an approach allows a description of the statistical nature of the plasma.

This paper will describe the NEET process in the framework of the formal theory of reactions. This approach is essentially based on a formal theory developed by Goldberger and Watson [18] and Cohen-Tannoudji *et al.* [19] to describe the properties of decaying states. The formalism is time dependent and consequently describes the time evolution of the coupling between the atom and the nucleus. This aspect is important in the present situation because an understanding of the NEET phenomenon in plasmas requires the comparison of different characteristic times. One time scale is that of the NEET process itself, and the others are associated with the hydrodynamic evolution of the plasma and the time duration of the LTE regime. Finally, such an approach has the added advantage of defining, in a consistent way, the widths and the atom-nucleus coupling in terms of the elementary interaction between the charged particles and the electromagnetic field. A more formal approach has been achieved [20,21]. This theoretical thermodynamic analysis, considering the nucleus in contact with a thermal reservoir, allows us to describe as a whole the interaction of the nucleus with its environment. Our approach separates this global calculation into a microscopic interaction, between the nucleus and its electronic cloud, and the thermodynamic aspect ruled by the plasma. That allows us to obtain a NEET rate more easily usable for applications in a laser experiment.

We will investigate the most relevant hydrodynamic parameters, such as charge state, density, and temperature, to obtain a good matching energy between the atomic and nuclear transitions for the excitation of the first isomeric state of  $^{235}\text{U}$ . As mentioned above, this calculation needs to take into account the complexity of the atomic spectra. When the spectrum becomes complex with many thermally available excited states, the number of configurations rises dramatically and statistical approaches must be used. In this case, an average-atom description may be attractive because of its simplicity. Nevertheless, it does not provide an accurate description of the atomic problem because the large number of configurations tends to split the average-atom transition into many components. Because each electron transition depends on the whole configuration, which may be very different from the average configuration, the average-atom formulation may fail to describe the atomic spectrum. However, in some cases, when the number of transitions is so high that the energy difference between two consecutive configurations is smaller than their widths, a strong overlap takes place. Then, a statistical approach using the distribution of the configurations around the average transition (obtained in the frame of the average-atom model) is a good approximation. From this approach, we will derive NEET rates as a function of density and temperature. At last, we will estimate the  $^{235m}\text{U}$  number created in a laser plasma.

## I. MICROSCOPIC PROBABILITY OF NEET

This section is devoted to the calculation of the probability of populating a long-lived nuclear excited state through its coupling with electronic transitions. The formalism presented here is an adaptation of the approach defined in Ref. [18] to study the properties of decaying states as a function of time. In this whole section, we will assume  $\hbar=1$ .

The point of departure here is the relation which exists between the time-dependent Schrödinger wave function  $|\Psi(t)\rangle$  and the Fourier transform  $[E+i\epsilon-H]^{-1}$  of the retarded Green's function. This relation has the simple form

$$|\Psi(t)\rangle = -\frac{1}{2i\pi} \lim_{\epsilon \rightarrow 0} \int_{-\infty}^{+\infty} \frac{1}{E+i\epsilon-H} e^{-iEt} |\Psi_i\rangle dE,$$

where the ket in the right-hand side corresponds to some initial condition at time  $t=0$ .

The probability amplitude  $J_{fi}(t)$  of a state  $|\Psi_f\rangle$  in the total wave function at time  $t$  is given by the scalar product

$$\begin{aligned} J_{fi}(t) &= \langle \Psi_f | \Psi(t) \rangle \\ &= -\frac{1}{2i\pi} \lim_{\epsilon \rightarrow 0} \int_{-\infty}^{+\infty} \langle \Psi_f | \frac{1}{E+i\epsilon-H} e^{-iEt} |\Psi_i\rangle dE. \end{aligned}$$

The probability  $P_f(t)$  that the system is in the final state “ $f$ ” at time  $t$  is then defined as

$$P_f(t) = \int |J_{fi}(t)|^2 \delta\rho_f(\epsilon) d\epsilon,$$

where  $\delta\rho_f(\epsilon)$  is the number of states  $f$  per energy unit.

Let us now define the total Hamiltonian which governs the time evolution of our system composed of the nucleus-atom system and the photon field. We write it in the form

$$H = H^{(0)} + V(\vec{r}),$$

where

$$V(\vec{r}) = V_C - \int \vec{j}(\vec{r}) \cdot \vec{A}(\vec{r}) d\vec{r},$$

$$H^{(0)} = H_N^{(0)} + H_A^{(0)} + H_\gamma^{(0)}.$$

The three Hamiltonians in  $H^{(0)}$  provide three complete sets of states describing separately the nucleus  $\{N\}$ , the atom  $\{A\}$ , and the photon field  $\{\gamma\}$ . The tensor product  $\{N\} \otimes \{A\} \otimes \{\gamma\}$  is assumed to be the product of eigenstates of the three systems in the absence of the coupling represented by the second term in the expression of  $H$ . The interaction  $V(\vec{r})$  is the residual Coulomb interaction  $V_C$  between the electrons and the nucleus plus a radiation coupling term. In the latter, the current  $\vec{j}(\vec{r})$  is the sum of the electronic and nuclear currents denoted as  $\vec{j}_e(\vec{r})$  and  $\vec{j}_n(\vec{r})$ , respectively, and  $\vec{A}(\vec{r})$  is the photon field associated with these two currents.

For our purpose, it is convenient to split the complete basis introduced above into two subsets by means of the well-known projector method. Denoting by  $P$  and  $Q$  the projectors in the spaces  $\{P\}$  and  $\{Q\}$ , the identity operator  $I$

becomes  $I=P+Q$ . It is straightforward to introduce these operators in the formalism developed in Ref. [18] and we will only quote the results here.

After some manipulations using standard operator algebra, we are led to the following expression:

$$J_{QP}(t) = -\frac{1}{2i\pi} \lim_{\epsilon \rightarrow 0} \int_{-\infty}^{+\infty} \frac{e^{-iEt} dE}{E+i\epsilon-E_Q} \langle \Psi_q | R_{QP}(E+i\epsilon) \times G_{PP}(E+i\epsilon) | \Psi_i \rangle, \quad (1)$$

representing the probability amplitude of any state  $\Psi_q \in \{Q\}$  in the total wave function at time  $t$ , starting from any initial  $\Psi_i \in \{P\}$ . This expression involves the so-called ‘‘reaction matrix’’  $R(z)$  defined by

$$R(z) = V + VQ \frac{1}{z - H_{qq}^0} QR(z),$$

and a Green’s operator  $G_{PP}(z)$  which is the inverse of operator  $P[z - H^{(0)} - R(z)]P$ . In this formalism, the operator  $P[H^{(0)} + R(z)]P$  can be interpreted as an effective Hamiltonian governing the propagation of the initial condition inside the space  $\{P\}$ . From the definition of  $R(z)$  it is clear that it takes into account the coupling with all the degrees of freedom in space  $\{Q\}$ . The analytic properties of the Green’s function and of  $R(z)$  have been studied in details by the authors of Ref. [18]. These properties are not only of great importance for the evaluation of the integrals as defined by Eq. (1) but they also provide valuable information on global physical quantities whose role is essential in the theory. The arguments of the authors in Ref. [18] are directly applicable to our case, and consequently we are content to summarize their findings.

Under general conditions on the potential, the matrix elements of  $G_{PP}(z)$  and  $R(z)$  are analytic functions in the entire  $z$  plane, except for real values of  $z$  in the continuous spectrum of  $H$ . Their domain of analyticity is defined here by the conditions  $0 < \arg(z) < 2\pi$ , assuming for simplicity that the continuum starts at zero. Another property concerns the analytic continuation of  $G_{PP}(z)$  for  $-2\pi < \arg(z) < 0$ . This function is expected to have singularities in the lower half plane which suggests that integral in Eq. (1) may be most easily evaluated by deforming the contour as described in Ref. [18]. The new contour is composed of small circles enclosing the poles and a contour, denoted by  $C_3$ , whose contribution can be neglected under reasonable assumptions. The evaluation of Eq. (1) is then reduced to a simple calculation of residues. This formal theory of decaying states is exploited in the simple model that we describe now.

The space  $P$  introduced above is spanned by the two states that are supposed to be coupled in the NEET process. We denote them as  $|\Psi_1\rangle = |\psi_1\varphi_1\rangle$  and  $|\Psi_2\rangle = |\psi_2\varphi_2\rangle$ . They are built with the two atomic excitations  $|\varphi_1\rangle$ , with energy  $\epsilon_1$ , and  $|\varphi_2\rangle$ , with energy  $\epsilon_2$  ( $\epsilon_1 > \epsilon_2$ ), and the two states  $|\psi_1\rangle$ , with energy  $E_1$ , and  $|\psi_2\rangle$ , with energy  $E_2$ , corresponding to the ground state and an isomeric state of the nucleus, respectively. For convenience, we designate by  $E_i^{\pm} = E_i + \epsilon_i$  the ener-

gies of the states  $|\Psi_i\rangle = |\psi_i\varphi_i\rangle$  and define the mismatch  $\delta$  between the nuclear and atomic transitions through the simple relation

$$\delta = E_1^+ - E_2^+ = \Delta\epsilon - \Delta E. \quad (2)$$

Now, since we are interested in the probability of populating a long-lived nuclear isomeric state (denoted here by  $\psi_2$ ), starting from the initial condition  $|\Psi_1\rangle = |\psi_1\varphi_1\rangle$ , we must calculate the amplitude given by Eq. (1) with any final state in  $Q$  containing  $\psi_2$ . It is denoted by  $|\Psi_q\rangle = |\psi_{2c}\rangle$  where the index  $c$  characterizes all open channels into which the state  $|\Psi_2\rangle = |\psi_2\varphi_2\rangle$  may decay through the matrix element  $\langle \psi_{2c} | R(E) | \Psi_2 \rangle$ . Thus, the probability amplitude defined by Eq. (1) is given, in this case, by the integral

$$J_{2c,1}(t) = \frac{1}{2i\pi} \lim_{\epsilon \rightarrow 0} \int_{-\infty}^{+\infty} \frac{dE}{E+i\epsilon-\epsilon_{2c}} \langle \psi_{2c} | R(E+i\epsilon) | \Psi_2 \rangle \times \langle \Psi_2 | G_{PP}(E) | \Psi_1 \rangle e^{-iEt}, \quad (3)$$

where  $\epsilon_{2c}$  denotes the energy of the final state. The total probability of populating the nuclear excited state is then given by summing over all possible final states:

$$P_2(t) = \sum_c \int |J_{2c,1}(t)|^2 \delta\rho_c(\epsilon_{2c}) d\epsilon_{2c}. \quad (4)$$

As mentioned above, the matrix elements of the Green’s function  $G_{PP}(E)$  are given by the inversion of the matrix defined by

$$\langle i | z - H | j \rangle = (z - E_i^{\pm}) \delta_{ij} - \langle \Psi_i | R(z) | \Psi_j \rangle.$$

In this simple model  $P$  is a two-dimensional space and, consequently, the inversion is straightforward. The result is

$$G_{ij}(z) = \frac{(-1)^{i+j}}{[z - E^+(z)][z - E^-(z)]} [(z - E_i^{\pm}) \delta_{ij} - \langle \Psi_i | R(z) | \Psi_j \rangle]. \quad (5)$$

Equation (5) can be expressed conveniently in term of physical quantities by means of the relation given in Ref. [18], namely,

$$\lim_{\epsilon \rightarrow 0} R_{ii}(E+i\epsilon) = \Delta_i(E) - i \frac{\Gamma_i(E)}{2}.$$

The real and imaginary parts reflect the fact that states in  $P$  are perturbed by their coupling with space  $\{Q\}$ . The quantity  $\Delta_i(E)$  is their energy shift and  $\Gamma_i(E)$  provides the rate of decay into the space  $\{Q\}$ . With these definitions, the quantities  $E^{\pm}(z)$  in Eq. (5) are given by

$$E^{\pm}(z) = \frac{1}{2} [E_M(z) \pm \sqrt{E_D^2(z) + 4|R_{12}(z)|^2}]$$

with

$$E_M(z) = 2 [E_{av} + \Delta_1(z) + \Delta_2(z)] - i[\Gamma_1(z) + \Gamma_2(z)],$$

$$E_D(z) = 2 [\delta + \Delta_1(z) - \Delta_2(z)] - i[\Gamma_1(z) - \Gamma_2(z)],$$

$$E_{av} = \frac{E_1 + E_2}{2}.$$

After inserting into Eq. (3) the matrix elements of the Green's function, given by Eq. (5), the probability amplitude finally takes the form

$$J_{2c,1}(t) = \frac{1}{2i\pi} \lim_{\epsilon \rightarrow 0} \int_{-\infty}^{+\infty} \frac{dE}{E + i\epsilon - \epsilon_{2c}} \frac{\langle \psi_{2c} | R(E + i\epsilon) | \Psi_2 \rangle}{[E - E^+(E)][E - E^-(E)]} \times \langle \Psi_2 | R(E) | \Psi_1 \rangle e^{-iEt}.$$

According to our general discussion, this integral is approximated by the residues at the poles located in the negative imaginary half plane. One pole is obviously  $\epsilon_{2c}$  and the others are solutions of the equations  $z_p^\pm = E^\pm(z_p^\pm)$  with  $-2\pi < \arg(z_p^\pm) < 0$ . In this application, the conditions

$$\frac{\Delta_i}{E_{av}} \ll 1,$$

$$\frac{\Gamma_i}{E_{av}} \ll 1,$$

$$\frac{2|R_{12}(E_{av})|}{|E_D(E_{av})|} \ll 1,$$

are satisfied. As a result, the two poles  $z_0^\pm$  closest to the real axis are given by

$$z_0^\pm \simeq E_{av} \pm \frac{\delta}{2} - i\frac{\Gamma^\pm}{2},$$

$$\Gamma^+ = \Gamma_1,$$

$$\Gamma^- = \Gamma_2.$$

Only the contribution of these three poles ( $\epsilon_{2c}, z_0^+, z_0^-$ ) is kept in the evaluation of the probability amplitude. After introducing this contribution into Eq. (4), we obtain the probability of exciting the isomeric level by NEET after time  $t$ . Although not essential, we make the reasonable assumption

$$R_{12}\left(E_{av} \pm \frac{\delta}{2}\right) \simeq R_{12}(E_{av})$$

in order to simplify the calculations. The final result is

$$P_{NEET}(\delta, t) = \frac{|R_{12}|^2}{\delta^2 + \left(\frac{\Gamma_1 - \Gamma_2}{2}\right)^2} \left[ 1 - e^{-\Gamma_2 t} + \frac{\Gamma_2}{\Gamma_1} (1 - e^{-\Gamma_1 t}) - \frac{\Gamma_2(\Gamma_1 + \Gamma_2)}{\delta^2 + \left(\frac{\Gamma_1 + \Gamma_2}{2}\right)^2} + \frac{2\Gamma_2 e^{-\frac{(\Gamma_1 + \Gamma_2)t}{2}} \cos(\delta + \phi)}{\sqrt{\delta^2 + \left(\frac{\Gamma_1 + \Gamma_2}{2}\right)^2}} \right] \quad (6)$$

with

$$\tan \phi = \frac{2\delta}{\Gamma_1 + \Gamma_2}.$$

This expression reaches an asymptotic value with a characteristic time given by the exponentials

$$\tau_{NEET} = \frac{1}{\Gamma_1} \quad \text{or} \quad \tau_{NEET} = \frac{1}{\Gamma_2}. \quad (7)$$

This asymptotic value reduces to the usual expression [2]

$$P_{NEET}(\delta, t = \infty) = P_{NEET}^\infty(\delta) = \frac{|R_{12}|^2}{\delta^2 + \left(\frac{\Gamma_1 + \Gamma_2}{2}\right)^2} \left(1 + \frac{\Gamma_2}{\Gamma_1}\right). \quad (8)$$

It is a Lorentzian shape as a function of the mismatch  $\delta$ , with a half-width

$$\Gamma = \frac{\Gamma_1 + \Gamma_2}{2}. \quad (9)$$

In this expression  $\Gamma_1$  and  $\Gamma_2$  are the widths of the electronic configurations which in this formalism are given by

$$\Gamma_i = 2\pi \sum_c \int |R_{2c,i}(\epsilon_c)|^2 \delta\rho_c(\epsilon_c) d\epsilon_c. \quad (10)$$

In the case of an isolated atom the main contribution to the widths comes from the radiative decay of the electron configurations, corresponding to the first-order term in the expansion of the reaction matrix, or more complicated processes such as the Auger effect (second order) for instance. In plasmas the situation may be quite different. There is another source of decay of the electron configurations due to their collisions with free electrons. As the density in the plasma is quite high, the widths associated with such collisions are much larger than those previously mentioned. Further expressions for these widths will be found below in Sec. IV.

It remains to derive the expression for the nondiagonal matrix element of  $R(E + i\epsilon)$ , which characterizes the coupling between the atomic and nuclear transitions. This is achieved by expanding the reaction matrix up to second order:

$$\begin{aligned} \langle \Psi_1 | R(E + i\epsilon) | \Psi_2 \rangle &= \langle \Psi_1 | V | \Psi_2 \rangle \\ &+ \langle \Psi_1 | V Q \frac{1}{E + i\epsilon - H_{qq}^{(0)}} Q V | \Psi_2 \rangle. \end{aligned} \quad (11)$$

Only the Coulomb interaction between the atom and the nucleus contributes to the first-order term. In the second-order term, only the radiation coupling contributes. For reasons given above, this matrix element is evaluated at  $E = E_{av}$  and, consequently, Eq. (11) reduces to

$$\begin{aligned} \langle \Psi_1 | R(E_{av} + i\epsilon) | \Psi_2 \rangle &= \langle \Psi_1 | V_C | \Psi_2 \rangle \\ &+ \int \frac{\omega d\omega}{4\pi R} \sum_{L,M,\pi} T_{e,(12)}^{LM\pi} T_{N,(21)}^{LM\pi*} \\ &\times \left[ \frac{1}{\frac{\delta}{2} + \omega_N - \omega} - \frac{1}{\frac{\delta}{2} + \omega_N + \omega} \right], \end{aligned} \quad (12)$$

where

$$T_{e,(12)}^{LM\pi} = \int \langle \varphi_1 | j_e(\vec{r}) A_{LM}^\pi(\vec{r}) | \varphi_2 \rangle d\vec{r},$$

$$T_{N,(21)}^{LM\pi} = \int \langle \psi_1 | j_N(\vec{r}) A_{LM}^{\pi*}(\vec{r}) | \psi_2 \rangle d\vec{r},$$

$$\omega_N = E_2 - E_1.$$

It is worth mentioning that in the point-nucleus approximation, the Coulomb term is exactly canceled by a static contribution coming from the second term. Notice also that, due to the presence of the energy mismatch  $\delta$ , expression (6) for  $P_{NEET}$  differs from the usual one obtained from the theory of internal conversion. To our knowledge, this aspect has not been accounted for in all previous calculations of the NEET process. A short appendix devoted to expression (12) is at the end of this paper.

The probability given by Eq. (6) is relevant to a plasma at LTE, characterized by its temperature  $T$  and density  $\rho$ . The quantities occurring in the definition of the NEET probability are well defined and depend upon  $\rho$  and  $T$ . Furthermore, by means of a statistical model one can estimate the number of atoms which contain the electronic configurations of interest for the NEET process. By taking this number as the initial condition, one obtains directly the number of excited nuclei at any later time (that does not exceed the time duration of the plasma). It is worth recalling that the atom-nucleus coupling is weak compared to the electronic and radiative processes and consequently has no significant influence on the equilibrium. We postpone the discussion to Sec. V where it is shown how this probability is used to derive an equivalent excitation rate in plasma, in spite of the fact that the expression for  $P_{NEET}$  in Eq. (6) contains an oscillatory term.

## II. ATOMIC CALCULATIONS

One of the most critical issues in the study of the NEET process is the mismatch  $\delta$  defined in Eq. (2) above, which characterizes the resonance. This quantity may vary greatly with the density and temperature of the plasma. An estimate of its average value can be obtained with a relativistic average-atom model. This model, first proposed by Rozsnyai [23], is based on an iterative method and assumes thermodynamic equilibrium. The model solves the Dirac-Fock equation for bound electrons, assuming the atom is in a spherical box with a radius dictated by the density. The self-consistent treatment starts with the relativistic Thomas-Fermi-Dirac model in the iterative procedure. The free electrons are treated statistically by means of the Fermi-Dirac distribution. The average-atom description is attractive because of its computational simplicity and because it provides a good representation of the plasma properties.

The average-atom model is the first step in extracting the region of interest in terms of density and temperature. For a given density and temperature, and for each electronic shell, the atomic calculations produce a binding energy, an ionization number, a population, and the associated electronic bound-state wave functions. These electronic wave functions are then used to build the many-electron wave function in the form of Slater determinants describing the average configuration. In such a configuration, the occupation numbers of electronic orbitals may be noninteger.

In the framework of the average-atom model, the expression for a transition energy is not straightforward: it can be obtained from the total energy of a real configuration constructed from a set of degenerate shells, with  $N_k$  being integer electrons in each shell, such as in Ref. [32],

$$E(C) = \sum_k U_k N_k + \frac{1}{2} \sum_{k\ell} V_{k\ell} N_k (N_\ell - \delta_{k\ell}),$$

where  $U_k$  contains the averaged kinetic energy and the electron-nucleus interaction in the  $k$ th orbital and  $V_{k\ell}$  contains the direct and the exchange coulomb interaction between an electron in orbital  $k$  and an electron in orbital  $\ell$ . The  $\frac{1}{2}$  coefficient prevents double counting of the correlations, and  $\delta_{k\ell}$  ensures the correct correlation between an electron in shell  $k$  with the  $N_k - 1$  others in the same shell.

Let us now consider the transition in which an electron from shell  $i$  is transferred to shell  $f$ . To get the transition energy, we define a spectator configuration  $C^*$  which is the total configuration less the two states in shell  $i$  and  $f$  involved in the transition. Then, by expressing the total configuration energy as a function of the spectator configuration energy, it is straightforward to estimate the energy difference between the configuration after and before the transition:

$$\Delta\epsilon = \bar{\epsilon}_i^0 - \bar{\epsilon}_f^0 + V_{if}(p_i - p_f) + \sum_k (V_{ik} - V_{fk})(N_k^* - \bar{N}_k^*),$$

where  $N_k^*$  (and  $\bar{N}_k^*$ ) is the population (and its mean value in the average atom model) of the  $k$  shell in the spectator's configuration,  $\bar{\epsilon}_i^0$  and  $\bar{\epsilon}_f^0$  are the level  $i$  and  $f$  energy in the average-atom model, and  $p_k$  is the occupation probability of

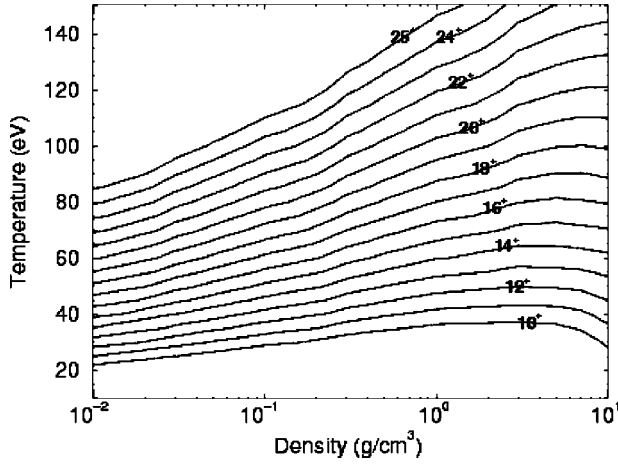


FIG. 1. Mismatch  $\bar{\delta}$  for the  $6d_{5/2}$ - $6p_{1/2}$  (left) and  $6p_{1/2}$ - $5d_{5/2}$  (right) transitions.

the  $k$  orbital given by the Fermi-Dirac statistics:

$$p_k = \frac{1}{1 + \exp\left(\frac{\bar{\epsilon}_k^0 - \mu}{kT}\right)},$$

where  $\mu$  is the chemical potential.

In the case of the average-atom model, the deviation from the mean value in the summation is zero and the expression of  $\Delta\epsilon$  reduces to

$$\bar{\Delta\epsilon} = \bar{\epsilon}_i^0 - \bar{\epsilon}_f^0 + V_{if}(p_i - p_f).$$

Following the definition (2), the average atom mismatch between the atomic and nuclear transitions is then obviously defined by

$$\bar{\delta} = \bar{\Delta\epsilon} - \Delta E. \quad (13)$$

We investigate relevant energy-matching atomic transitions in the case of the isomeric level of  $^{235}\text{U}$ , located at 76.8 eV. We have plotted in Fig. 1 the isovalues of  $\bar{\delta}$  in the density-temperature map for the  $6d_{5/2}$ - $6p_{1/2}$  and  $6p_{1/2}$ - $5d_{5/2}$  atomic transitions of a uranium ion. Two valleys relative to a set of density-temperature points, corresponding to the  $6d_{5/2}$ - $6p_{1/2}$  and  $6p_{1/2}$ - $5d_{5/2}$  transitions under matching conditions ( $\bar{\delta} \sim 0$ ), can be extracted. It is clear that the best matching can be realized under different conditions of temperature density. Figure 2 represents the isovalues of uranium charge state in the density-temperature map. The best matchings for the  $6d_{5/2}$ - $6p_{1/2}$  and  $6p_{1/2}$ - $5d_{5/2}$  transitions are, respectively, around  $Z^* = 21^+$  and  $Z^* = 11^+$ . However, optimizing the mismatch is not the only criterion for NEET transitions. One must also look at the probability to find at least one electron in the initial electronic shell and one hole in the final electronic shell. Figure 3 shows the occupation number of the  $6d_{5/2}$ ,  $6p_{1/2}$ , and  $5d_{5/2}$  atomic shells, as a function of density, along both valleys of minimum mismatch in the  $(\rho, T)$  map. The  $6d_{5/2}$ - $6p_{1/2}$  transition seems to be more favorable than

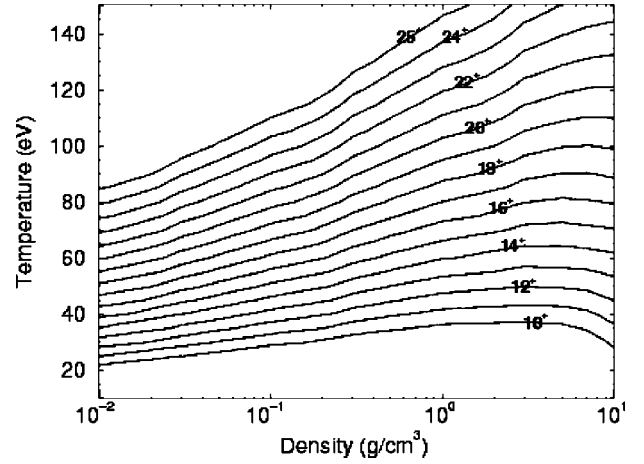


FIG. 2. Average charge state of LTE uranium plasma across the  $(\rho, T)$  plane.

the other one. Furthermore, the occupation number increases with density, thus implying that the NEET rate may vary along the zero mismatch valley.

### III. THE ATOM-NUCLEUS MATRIX ELEMENT

The coupled atom-nucleus matrix elements  $|R_{12}|^2$  involved in Eq. (8) are also calculated in the framework of the average-atom model. For a nuclear transition  $EL$ , between nuclear states with spins  $j_g$  and  $j_e$ , we have (a more detailed development is given in the Appendix)

$$|R_{12}(\delta)|^2 = 4\pi\alpha\omega_N^2 \left(\omega_N + \frac{\delta}{2}\right)^{2L} \frac{2j_e + 1}{L^2[(2L+1)!]^2} \times \begin{pmatrix} j_g & j_e & L \\ 1/2 & -1/2 & 0 \end{pmatrix}^2 |R_{n_1\kappa_1 n_2\kappa_2}|^2 B(EL),$$

where  $\alpha$  is the fine-structure constant and  $R_{n_1\kappa_1 n_2\kappa_2}$  is the radial electronic matrix element for an electric transition of multipolarity  $L$  defined by

$$R_{n_1\kappa_1 n_2\kappa_2} = \int \{L(g_1g_2 + f_1f_2)h_L(\omega_N r) + [(\kappa_1 - \kappa_2 - L)g_1f_2 + (\kappa_1 - \kappa_2 + L)f_1g_2]h_{L-1}(\omega_N r)\} dr$$

Here  $\kappa_1$  and  $\kappa_2$  represent the relativistic quantum numbers,  $g_1, g_2, f_1$ , and  $f_2$  are the large and small radial components of the initial and final atomic wave functions, and  $h_L$  is the Hankel function of the first kind.

$B(EL)$  is the reduced nuclear matrix element rate, in Weiskopf units (W.u.). For the  $^{235}\text{U}$  transition, from  $j_g = 7/2^-$  to  $j_e = 1/2^+$ , we deduced from the internal coefficient  $\alpha_{E3}$  given by Band and Trzhaskovskaya [24] and from the lifetime of the isomer  $t_{1/2}$

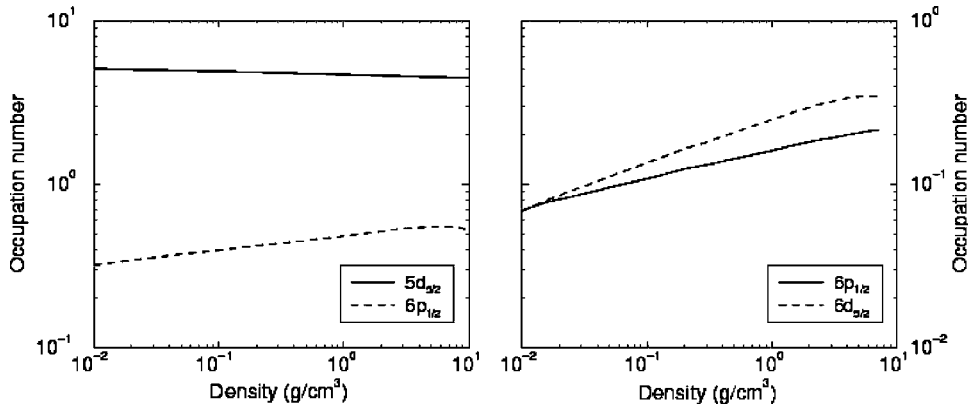


FIG. 3. Average atom occupation numbers vs density along the minimum mismatch valleys of  $6p_{1/2}-5d_{5/2}$  (left) and  $6d_{5/2}-5p_{1/2}$  (right) transitions in the  $(\rho, T)$  map.

$$\begin{aligned}
 B(E3) &= \frac{1}{2j_g + 1} | \langle j_e || M_N(E3) || j_g \rangle |^2 \\
 &= 1.5 \times 10^{-19} \left( \frac{197}{E(\text{MeV})} \right)^7 \frac{\ln 2}{t_{1/2}(1 + \alpha_{E3})} \\
 &= 0.069 \text{ W.u.}
 \end{aligned}$$

The coupled atom-nucleus matrix element is a slowly varying function of the density along the resonance valley. Its value is  $\approx 1.9 \times 10^{-18} \text{ eV}^2$  for the  $6d_{5/2}-6p_{1/2}$  transition and  $\approx 0.6 \times 10^{-18} \text{ eV}^2$  for the  $6p_{1/2}-5d_{5/2}$  one.

The matrix element  $|R_{12}|^2$  is larger when the initial and final levels are in the same layer (as defined by the electronic principal quantum number  $n$ ) because the wave function overlap is larger. Moreover, Fig. 3 shows that occupation numbers are more favorable for the  $6d_{5/2}-6p_{1/2}$  transition than for the  $6p_{1/2}-5d_{5/2}$  one. Therefore, we will concentrate on the  $6d_{5/2}-6p_{1/2}$  transition.

#### IV. WIDTHS AND CHARACTERISTIC TIMES

Different widths and characteristic times are of paramount importance when dealing with the NEET process. According to the above calculations, the evolution of a nucleus-atom system with an initial electronic configuration favorable to the NEET process takes place within a very short time frame. The NEET probability reaches an asymptotic maximum within a characteristic time given by the collision widths, as given by Eq. (7). Another important feature is the variation of the transition energy mismatch. Indeed, we have to check that the mismatch does not change significantly during the evolution of the system leading to the excitation of the nucleus by the NEET process.

##### A. Collision time

The general expression for the electronic configuration width (10) may be expressed in the particular case of continuum electron collisions with the help of the general work of Baranger [25], and the more detailed applications described in Refs. [26,27]. The collision width of the atomic configuration may be written as

$$\Gamma_{col} = \alpha^2 \hbar c \frac{4\sqrt{2}}{3\sqrt{3}} \pi^{3/2} N_e \sqrt{\frac{m_e c^2}{kT_e}} [ \langle \phi_1 | r^2 | \phi_1 \rangle + \langle \phi_2 | r^2 | \phi_2 \rangle ],$$

where  $N_e$  is the electron density, and  $\phi_1$  and  $\phi_2$  are the wave functions of the two atomic shells involved. This formula is

obtained in the impact approximation assuming that the collision time is much smaller than the time required for an atomic transition. In addition, the collisional width uses a Maxwellian electron distribution. As the electronic collision is the fastest process involved in the equilibration of the electronic populations, this leads to a collision time expressed as

$$\tau_{col} = \frac{\hbar}{\Gamma_{col}}.$$

For the two atomic transitions of uranium, Fig. 4 shows the variations of the collision width along the valley of perfect matching. These widths correspond to characteristic times always smaller than  $10^{-13} \text{ s}$ .

##### B. Hydrodynamic calculations

The main advantage in studying the NEET effect in a plasma is the large number of readily formed atomic configurations with an electron in the upper level and a hole in the lower one with  $\bar{\delta} \approx 0$  in the appropriate temperature-density regimes. This condition can only be obtained for long durations in a laser-heated plasma. Therefore, we will restrict ourselves to these types of plasmas as they are the most convenient for the desired range of temperatures.

The main drawback is the highly nonstationary nature of those plasmas. Therefore, we need to follow the time dependence of different parameters. We have made such calculations using a radiative hydrodynamic Lagrangian bidimen-

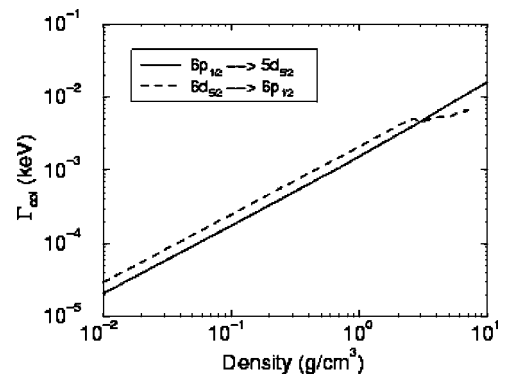


FIG. 4. Collision width as a function of density along the valley  $\bar{\delta}=0$ .

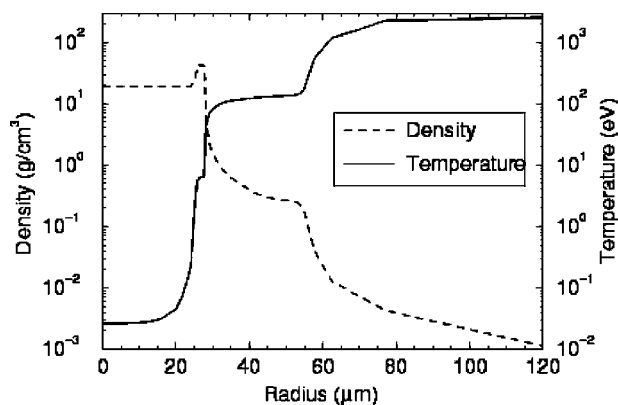


FIG. 5. Temperature and density profiles in uranium at  $10^{14}$  W/cm $^2$ .

sional code simulating the laser matter interaction. The plasma is simulated by a single fluid with nonhomogeneous ionic and electronic temperatures. These need not be at thermodynamic equilibrium with the radiation. In addition to the mass, momentum, ionic, and electronic energy conservation laws, the code solves the radiative intensity transport equations, with a coupling term linking radiative and electronic equations, to simulate photon absorption and emission in matter. The electron heat flux is calculated using the heat conductivity given by Spitzer [28]. This flux must not exceed the free-streaming limit

$$f_{lim} n_e T_e \sqrt{\frac{T_e}{m_e}},$$

where  $f_{lim}$  is an adjustable parameter taken at 0.13 in our calculations. The calculation presented here corresponds to a laser intensity of  $10^{14}$  W/cm $^2$ , with a wavelength  $\lambda = 1.06$   $\mu$ m, a pulse duration of 1 ns, a spot size of 1 mm in diameter, and a very sharp shape (nearly similar to a square pulse). The intensity was optimized to get the LTE area in favorable conditions for the NEET process associated with the  $6d_{5/2}-6p_{1/2}$  transition.

The temperature and total density profiles relative to the maximum beam power are plotted in Fig. 5, as a function of target materia depth. The laser beam penetrates into the target from the right, where the matter is hotter. The laser-matter interaction occurs deeper and deeper in the target until critical density has been reached. The critical density, at which the laser light is reflected, is inversely proportional to the square of the laser wavelength. For the low density in this area, electrons, ions, and radiation are in a nonthermodynamic equilibrium state with three different temperatures. At higher density and lower temperature, the LTE regime takes place in the absorption-reemission area (just beyond the critical density). This reemission zone is heated by the successive absorptions and reemissions, inside the reemission zone, of the soft x rays first emitted in the conversion layer where the laser energy is absorbed. Usually, most of the studied laser plasmas are in the nonlocal thermodynamic equilibrium regime. The high opacity of the LTE area due to its high density precludes accurate or detailed observations

of events occurring in the absorption-reemission area. However, the reemission zone has a much larger mass than the conversion layer and that is why it is of more interest in our study. The laser characteristics, in terms of energy, spot size, and duration, have been chosen to optimize the size of the LTE area, where most NEET effects occur.

These hydrodynamic calculations allow us to follow the variation of plasma temperature and density. As the mismatch depends on the temperature and density, it is then possible to know the evolution of the mismatch in the reemission zone as a function of time.

### C. Mismatch variations

The main parameter influencing the microscopic NEET probability is the energy mismatch  $\delta$ . The validity of the whole calculation performed in Sec. I, especially the NEET probability as a function of time given by Eq. (6), implies that the mismatch variation is small during the time  $\tau_{NEET}$  needed to reach the asymptotic value. This variation is

$$\frac{d\delta}{dt} \tau_{NEET} = \frac{d\delta \hbar}{dt \Gamma}.$$

The amplitude of these variations must be less than the half-width  $\Gamma$  of the Lorentzian of  $P_{NEET}^\infty$  given by the Eq. (9) for the asymptotic value to be stationary. Therefore the following condition must be met:

$$\frac{d\delta \hbar}{dt \Gamma} \ll \Gamma \Leftrightarrow \frac{d\delta}{dt} \ll \frac{\Gamma^2}{\hbar}. \quad (14)$$

The atomic evolution is controlled by the plasma expansion. In a laser plasma, the mismatch variations are induced by the variations of the density and the temperature. We use a hydrodynamic calculation to get the mismatch variation. The derivative of the mismatch over time is

$$\frac{d\delta}{dt} = \frac{\partial \delta}{\partial \rho} \frac{\partial \rho}{\partial t} + \frac{\partial \delta}{\partial T} \frac{\partial T}{\partial t}.$$

The derivatives of the mismatch over density or temperature have been obtained with the average-atom model. Density and temperature derivatives over time are calculated by the hydrodynamic model described in Sec. IV B. The time variation of the derivative of the mismatch is shown in Fig. 6. In the region of interest, the derivative of the mismatch over the time satisfies the relation

$$\left| \frac{d\delta}{dt} \right| \leq 1 \text{ eV/ns.}$$

So we can deduce from Eq. (14) a condition on the half-width:

$$\Gamma > 10^{-3} \text{ eV.}$$

For both transitions of interest, Fig. 4 shows that this condition is always fully met. This implies that the stationary conditions required by the calculations of Sec. I are verified. Thus, the microscopic NEET probability given by Eq. (6) may be used. Figure 7 shows the evolution in time of the

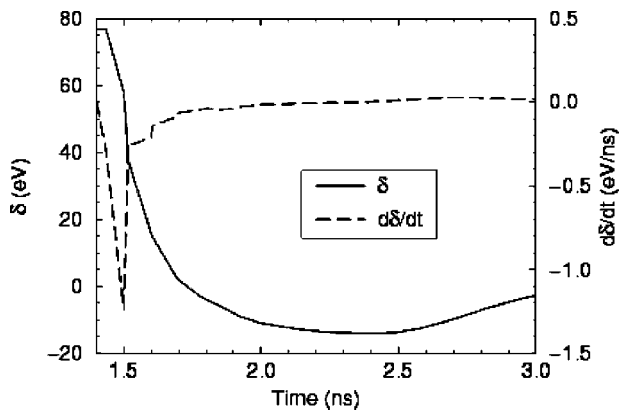


FIG. 6. Mismatch and its derivative as a function of time for  $6d_{5/2}-6p_{1/2}$  transitions in the region of interest.

microscopic NEET probability under stationary thermodynamic conditions. Moreover, the asymptotic value has been reached before the mismatch and other atomic physics related quantities have changed. Therefore, we are able to use the asymptotic expression (8) in our evaluations of the NEET rate in the plasma.

## V. NEET EXCITATION RATE IN A PLASMA

### A. The NEET rate

The different characteristic times described in Sec. IV allow us to express a NEET rate in the plasma. Since the microscopic NEET time is much less than the mismatch variation characteristic time, it is possible to use the asymptotic value of the microscopic NEET probability given by Eq. (8). Furthermore, the hydrodynamic conditions vary even more slowly, so that the NEET rate can be evaluated using stationary thermodynamic conditions.

The probability of transition by the NEET process, from an initial atomic configuration  $\alpha$  to a final atomic configuration  $\beta$ , can be expressed as

$$\lambda_{\alpha} P_{NEET}^{\infty}(\delta_{\alpha\beta}),$$

where  $\lambda_{\alpha}$  is the initial configuration decay rate, which, at LTE, is also its creation rate. It is directly related to the width of the initial configuration by

$$\lambda_{\alpha} = \frac{\Gamma_{\alpha}}{\hbar}.$$

From the asymptotic NEET probability (8), the NEET rate of isomer creation may be written as a sum over all initial and final configurations:

$$\lambda^{NEET}(\rho, T_e) = \sum_{\alpha, \beta} P_{\alpha}(\rho, T_e) \lambda_{\alpha} P_{NEET}^{\infty}(\delta_{\alpha\beta}).$$

where  $P_{\alpha}$  is the initial configuration probability.

At LTE  $P_{\alpha}$  is given by

$$P_{\alpha}(\rho, T) = \frac{1}{Z_G} D_{\alpha} \exp\left(-\frac{E_{\alpha} - \mu \sum_{i=1}^{k_{max}} P_{\alpha i}}{kT}\right),$$

where  $p_{\alpha i}$  is the population of the  $i$  bound shell of the ion with the configuration  $\alpha$ .  $D_{\alpha}$  is the degeneracy of the configuration,  $E_{\alpha}$  its energy,  $k_{max}$  is the total number of occupied shells, and  $Z_G$  is the normalization factor. If we substitute the NEET transition probability of Eq. (8), the NEET rate becomes

$$\lambda^{NEET}(\rho, T_e) = \sum_{\alpha, \beta} P_{\alpha}(\rho, T_e) \frac{\Gamma_{\alpha}}{\hbar} \frac{|R_{\alpha\beta}(\delta)|^2}{\delta_{\alpha\beta}^2 + \left(\frac{\Gamma_{\alpha} + \Gamma_{\beta}}{2}\right)^2} \left(1 + \frac{\Gamma_{\beta}}{\Gamma_{\alpha}}\right).$$

In this last expression, every single real configuration is taken into account. The huge number of different configurations precludes any exact calculation and so only a statistical approach can be used to describe the complexity of the atomic spectrum. Under LTE conditions, the atomic-configuration distribution around the average atom configuration corresponds to a mismatch distribution  $\delta_{\alpha\beta}$  around the average atom mismatch  $\bar{\delta}$  given by Eq. (13). As the number of configurations is very large, the transitions are closely spaced and a strong overlap takes place. So, we can replace the discrete summation over the real configurations by an integral over a statistically broadened averaged transition approximated by a Gaussian distribution [29–33]. The variations of the matrix element and the widths as a function of the mismatch are assumed to be small and their values are calculated within the framework of the average-atom model for an electronic transition, from shell 1 to shell 2 ( $6p_{1/2}$

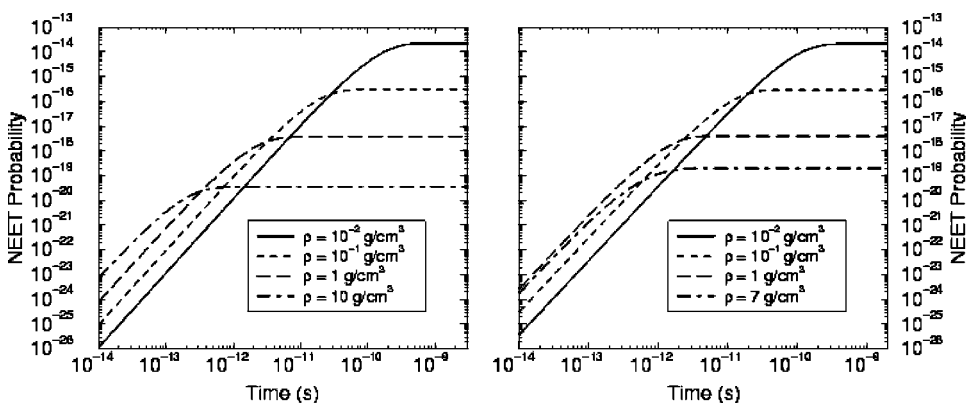
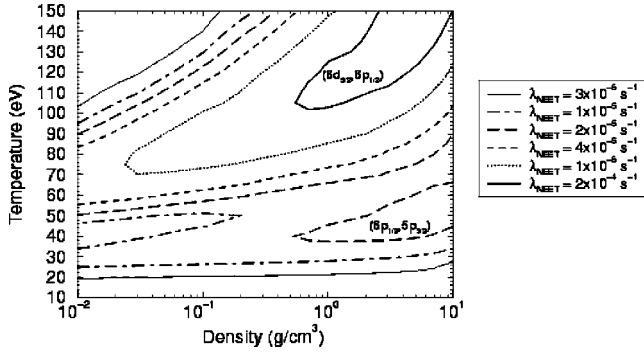


FIG. 7. Microscopic NEET probability vs time for the resonant  $6p_{1/2}-5d_{5/2}$  (left) and  $6d_{5/2}-6p_{1/2}$  (right) transitions.


 FIG. 8. Rate of NEET across the  $(\rho, T)$  plane.

$-5d_{5/2}$  or  $6d_{5/2}-6p_{1/2}$ ). Finally, we assume that the statistically averaged transition lies between two atomic shells whose populations are given by the average-atom model.

Thus we can write

$$\lambda^{NEET}(\rho, T_e) = D_1 p_1 (1 - p_2) \int_{-\infty}^{+\infty} \frac{\Gamma_1}{\hbar} \frac{1}{u^2 + \left(\frac{\Gamma_1 + \Gamma_2}{2}\right)^2} \times \left(1 + \frac{\Gamma_2}{\Gamma_1}\right) \frac{|R_{12}(\bar{\delta})|^2}{\sqrt{2\pi\sigma^2}} e^{-(u - \bar{\delta})^2 / 2\sigma^2} du,$$

where  $D_i$  is the  $i$  shell degeneracy and  $p_i$  its occupation probability.

The energy variance  $\sigma$ , defined in Ref. [31], describes the dispersion of the electronic transition energy of real configurations around the average-atom value:

$$\sigma^2 = \sum_{i,j} \left(\frac{\partial \bar{\delta}}{\partial p_i}\right)_{p_j} \left(\frac{\partial \bar{\delta}}{\partial p_j}\right)_{p_i} \langle \Delta p_i \Delta p_j \rangle.$$

The order of magnitude of the energy variance is around a few eV, much larger than the collision widths  $\Gamma_1$  and  $\Gamma_2$ . Therefore, the integral above can be approximated by its value at  $u=0$ . The final NEET rate is

$$\lambda^{NEET}(\rho, T_e) = \frac{2\pi}{\hbar} D_1 p_1 (1 - p_2) |R_{12}(\bar{\delta})|^2 \frac{1}{\sqrt{2\pi\sigma^2}} e^{-\bar{\delta}^2 / 2\sigma^2}. \quad (15)$$

This rate does not depend on the collision widths  $\Gamma_1$  and  $\Gamma_2$ . It can be easily understood if one considers that these widths are those of the individual atomic transitions. They are completely merged within the statistical average transition characterized by the single width  $\sigma$ .

Figure 8 shows the map of the NEET rate of the excitation of the first isomeric state of  $^{235}\text{U}$ . We clearly see the two favorable zones for the NEET effect corresponding to  $6p_{1/2}-5d_{5/2}$  and  $6d_{5/2}-6p_{1/2}$  electronic transitions in agreement with Ref. [16]. For a given density, the variation of  $\lambda^{NEET}$  as a function of the temperature shows important fluctuations. For instance, at  $1 \text{ g/cm}^3$  the NEET rate goes from  $10^{-6}$  to  $2 \times 10^{-4} \text{ s}^{-1}$  depending on the temperature. For a given temperature, the variation versus the density of the NEET rate may be as important. These variations closely follow the

evolution of the mismatch shown in Fig. 1. The intensity of the  $\lambda^{NEET}$  is then given by the probability to find an electron on the upper shell and a hole in lower shell.

In a plasma, other processes may compete with the NEET mechanism: resonant photon absorption, inelastic electron scattering, and inverse internal conversion (also known as nuclear excitation by electron capture). We have made estimates of these different processes in the thermodynamic region where the NEET calculation was performed.

The first mechanism, resonant photon absorption, strongly depends on the radiation temperature. At the resonance, for a photon energy of 76.8 eV, the cross section is about  $10^{-33} \text{ cm}^2$ . With a Maxwellian photon distribution around 100 eV, the resulting photoexcitation rate is extremely low, about  $6 \times 10^{-25} \text{ s}^{-1}$ .

The second mechanism, the so-called inelastic electron excitation, depends on the electron energy and, thus, on the plasma temperature. In Ref. [16], the inelastic electron rate was estimated, in the framework of the Born approximation, as  $10^{-16} \text{ s}^{-1}$  for an electron temperature of 100 eV. However, in a laser-created plasma, the electric field of the laser beam may cause electrons in the target plasma to oscillate and the laser beam can couple to collective modes. The thermalization of this absorbed energy is far from being complete and the creation of suprathermic electrons is possible. A temperature may be associated with that electronic component, depending on the intensity and the wavelength of the laser light. An empirical expression for this temperature  $T_e^{hot}$  was proposed by different authors [34,35]:

$$T_e^{hot} \approx 10^{-5} (I_L \lambda_L^2)^{0.4},$$

where  $T_e^{hot}$  is expressed in keV,  $I_L$  is the laser intensity in  $\text{W/cm}^2$ , and  $\lambda_L$  its wavelength in  $\mu\text{m}$ .

These suprathermic electrons can excite energy levels beyond the isomeric state. With an intensity of  $10^{14} \text{ W/cm}^2$  and a wavelength of  $1.06 \mu\text{m}$ , the suprathermic electronic temperature lies around 4 keV. 10% of these electrons have an energy greater than 13 keV allowing the excitation of the level located at 13 keV (with spin and parity  $3/2^+$ ). This level decays down to the isomer with a 100% branching ratio. However, the excitation of the 13 keV level by an  $M2$  transition is also difficult and its contribution to the excitation rate of the isomer is very low.

The last excitation mechanism, NEEC, is the most efficient of these other excitation mechanisms. By using the microreversibility at LTE, it is possible to extract a NEEC rate from the internal conversion rate. This last rate needs to be modified by using the electron occupation probabilities on each atomic shell allowing internal conversion. A more detailed treatment of this process will be given in a later publication [36]. On the whole density-temperature map of interest, the NEEC rate never exceeds  $10^{-6} \text{ s}^{-1}$ , which is smaller than our calculated NEET rate.

## B. Validity of the NEET rates in a plasma

As mentioned above, our NEET rates are valid at the thermodynamic equilibrium. A question arises regarding the validity of the LTE hypothesis in the plasma region of such

densities and temperature. During laser-plasma interaction, atoms in the reemission zone are heated by thermal x rays coming from the conversion area where the laser energy is absorbed. This reemission zone is optically thick for x rays and therefore radiates blackbody radiation. The temperature evolves slowly inside the reemission zone which can be considered in equilibrium with a thermostat whose temperature is given by the absorbed laser energy. To delimitate this area, a LTE criterion was proposed by Griem [38,39], using the ionization energy  $E_\zeta$  of charge  $\zeta$ :

$$n_e \geq (1 \times 10^{14} \text{ cm}^{-3}) T_e^3 \left( \frac{E_\zeta}{T_e} \right)^{5/2}.$$

It shows that for a temperature greater than 30 eV and a density greater than 0.1 g/cm<sup>3</sup>, the LTE hypothesis is valid over the whole density-temperature map covered in the Fig. 8.

The Thomas-Fermi approximation used to calculate the free electron density in the averaged atom model may be not accurate for temperatures below 40 eV. This error is difficult to quantify. However, it is irrelevant in our study because the maximum of the NEET rate occurs at a temperature higher than 40 eV.

The comparison of the calculated NEET rates with experimental data is difficult because in each case we need to describe the plasma dynamics with a good accuracy. The excitation rate greater than 1 s<sup>-1</sup>, obtained by a Japanese group [12], is clearly too high to be reproduced by our calculations. However, studies done in Refs. [13,40] show that the measured electrons in such an experiment may originate from a purely solid-state physics effect. On the other hand, the experimental limit on the excitation rate 10<sup>-3</sup> s<sup>-1</sup>, obtained in Refs. [14,15], is consistent with our calculations.

The NEET rate is low and never greater than 10<sup>-3</sup> s<sup>-1</sup>. The number of isomers produced in such an experiment is difficult to predict because it depends on the description of the temperature and density of the plasma a long time after the laser pulse. In hydrodynamic codes, the cooling down of the plasma is hard to describe [37], and precise calculations are currently out of reach. However, we can estimate the number of isomers created in the thermodynamic conditions described in Sec. IV B.

### C. Isomer production

The global rate of isomer creation per time unit is obtained by integrating the local NEET isomer creation rate over the whole plasma volume:

$$\frac{dN_{iso}}{dt} = \int \frac{dn_{iso}(\vec{r})}{dt} d\vec{r}$$

with

$$\frac{dn_{iso}(\vec{r})}{dt} = \lambda_{NEET}(\rho, T) n_{U5}(\vec{r})$$

and  $n_{U5}(\vec{r})$  is the uranium density.

Each point in the plasma is well characterized by a density  $\rho$  and a temperature  $T$ . For a  $(\rho, T)$  couple there corre-

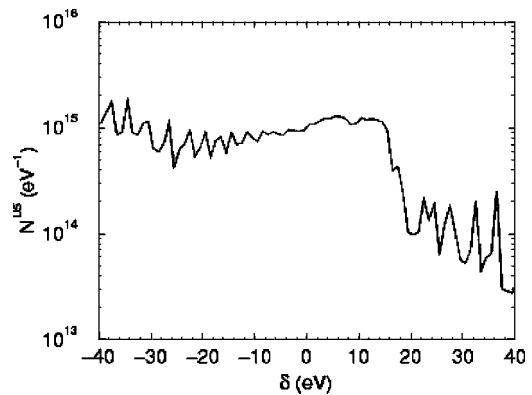


FIG. 9. Number of <sup>235</sup>U per mismatch unit vs  $\delta$  for one laser beam.

sponds a  $\delta$ -mismatch value. Therefore, we can replace the variable  $\vec{r}$  by  $\bar{\delta}$  under the integral. So, we can write

$$\frac{dN_{iso}}{dt} = \int \lambda_{NEET}(\rho, T) N_{U5}(t, \bar{\delta}) d\bar{\delta}$$

if we define  $N_{U5}(t, \bar{\delta})$  as the number of <sup>235</sup>U per mismatch unit in the whole plasma volume. The number is shown in Fig. 9 as a function of the mismatch  $\bar{\delta}$ . The number of uranium atoms per mismatch unit, around  $\bar{\delta}=0$ , is nearly constant within a  $\sigma$  range of few eV and amounts to about 10<sup>15</sup> eV<sup>-1</sup>. This  $\bar{\delta}$ -dependent law suggests that the use of the average-atom model is justified. As  $N_{U5}(t, \bar{\delta})$  is independent of  $\bar{\delta}$  around  $\bar{\delta}=0$ , we can integrate equation over  $\bar{\delta}$  by factorizing  $N_{U5}$  out of the integral. So we can write:

$$\frac{dN_{iso}}{dt} = \frac{2\pi}{\hbar} D_1 p_1 (1 - p_2) |R_{12}(\bar{\delta}=0)|^2 N_{U5}(t, \bar{\delta}=0).$$

Using  $D_1 p_1 (1 - p_2) |R_{12}|^2 \approx 10^{-19}$  eV<sup>2</sup>, we get

$$N_{iso} \approx 10^{12} \text{ s}^{-1} \times \Delta t,$$

where  $\Delta t$  is the duration of the plasma, assumed be around 10 ns, for a laser duration of 1 ns. This gives a number of isomers created during the plasma expansion which never exceeds 10<sup>4</sup>, and a uranium isomer activity lower than 4 Bq at the beginning of the measurement. A successful measurement requires an isomer number two or three orders of magnitude higher. Even by modifying the experimental conditions, such as the size of laser spot or the laser intensity, reaching such a number seems unlikely.

All this work has been done assuming a direct laser attack on a uranium target. We can also imagine an indirect drive, in a uranium-gold cavity, to make the radiative temperature confined in the *hohlraum* for a time long enough to produce the NEET process. A temperature of a few hundred eV can easily be reached with a laser power lower than for a direct attack. Such a calculation can be performed to improve the understanding further of NEET.

Whatever the experimental technics used, the  $^{235}\text{U}$  NEET rate is very low. This is mainly due to the nuclear part of the matrix element. To test our model, we need to find a candidate with a more favorable nuclear transition. In this context, we considered the excitation of the first state of  $^{193}\text{Pt}$  located at 1.642 keV. It decays down to the ground state by an  $M1$  transition ( $t_{1/2}=9.7$  ns). We found that the  $5s_{1/2}-4s_{1/2}$  atomic transition is resonant for a LTE plasma temperature around 1 keV or 2 keV, giving a NEET rate greater than  $10^6$  s $^{-1}$ . However, the difficulty lies in detecting the excited platinum nucleus as it decays through a strongly converted transition whose lifetime is nearly the same as the plasma. Moreover, we need to create a LTE plasma at about 1 keV. In the future, with the advent of the intense lasers, the creation of such a plasma will certainly become feasible.

### CONCLUSION

We have described the microscopic dynamics of the NEET probability and shown, for the first time, to our knowledge, that the vertex describing the coupling between the atomic and nuclear transition for the NEET effect is different from that of internal conversion. For a dense plasma, this microscopic NEET probability reaches an asymptotic value after a very short time, which is the characteristic time associated with the free electrons collisions with the atom. This asymptotic probability is exactly the NEET probability usually found in a more simple model. This NEET probability is then used to derive an excitation rate in the plasma, calculated on a  $(\rho, T)$  map, under the hypothesis of local thermodynamic equilibrium. This is made possible by the slowly varying thermodynamic conditions and atom physics

description. The NEET rate varies sensitively with thermodynamic conditions. We have presented a study of the excitation of the first isomeric state of  $^{235m}\text{U}$  by the NEET effect. The maximum isomer production areas are around 110 eV and 35 eV for a density of 0.1 g/cm $^3$ . They correspond to the resonant atomic transitions  $6d_{5/2}-6p_{1/2}$  and  $6p_{1/2}-5d_{5/2}$ . However, the excitation rates for  $^{235}\text{U}$  are too low to perform an experiment and we propose to carry on this study with  $^{193}\text{Pt}$ , which seems to be a more promising candidate.

### ACKNOWLEDGMENTS

This work was performed in part under the auspices of U.S. Department of Energy by the University of California, Lawrence Livermore National Laboratory under Contract No. W-7405-Eng-48, and at the CEA in Bruyères-le-Château. The authors gratefully acknowledge helpful discussions with J. Becker and A. Decoster.

### APPENDIX

According to Eq. (12), the atom-nucleus coupling can be expressed as

$$\langle \Psi_1 | R(E_{av} + i\epsilon) | \Psi_2 \rangle = -8 \int d\omega \omega^2 \sum_{L,M,\pi} T_{e,(12)}^{LM\pi} T_{N,(21)}^{LM\pi*} \left[ \frac{1}{\omega^2 - \left(\frac{\delta}{2} + \omega_N\right)^2} \right].$$

Only electric transitions are considered in the present application and consequently this matrix element becomes

$$-8 \int d\omega \omega^2 \frac{\sum_{L,M} \int \langle \varphi_1 | \vec{j}_e(\vec{r}) A_{LM}^E(\vec{r}) | \varphi_2 \rangle d\vec{r} \int \langle \varphi_1 | \vec{j}_N(\vec{r}') (A_{LM}^E)^*(\vec{r}') | \psi_2 \rangle d\vec{r}'}{\omega^2 - \left(\frac{\delta}{2} + \omega_N\right)^2}. \tag{A1}$$

The coefficients  $A_{LM}^E(\vec{r})$  are the electric components in the multipole expansion of the potential vector:

$$A_{LM}^E(\vec{r}) = \frac{1}{\omega \sqrt{L(L+1)}} \vec{\nabla} \times \vec{L} j_L(\omega r) Y_{LM}(\vec{\Omega}).$$

Inserting this expression in Eq-(A1), the integration over  $\omega$  can be performed using the identity given in Ref. [22]:

$$\int_0^\infty \frac{1}{\omega^2 - \beta^2} j_L(\omega r) j_L(\omega r') d\omega = i \frac{\pi}{2\beta} j_L(\beta r_<) h_L(\beta r_>) - \frac{\pi}{2(2L+1)\beta^2} \frac{r_<^L}{r_>^{L+1}},$$

where  $\beta = \omega_N + \delta/2$ ,  $r_<$  is the smaller of  $r$  and  $r'$ , and  $r_>$  the larger.

Now, if we make the point-nucleus approximation, the integrations over the volumes of the nucleus and atom can be performed separately. Furthermore, as previously mentioned, the second term of Eq. (11) cancels exactly the static contribution of the coulomb interaction. Thus within such an approximation we obtain

$$\begin{aligned} \langle \Psi_1 | R(E_{av} + i\epsilon) | \Psi_2 \rangle &= -4i \frac{\pi}{\beta L(L+1)}. \\ \sum_{L,M} \int \langle \varphi_1 | \vec{j}_e(\vec{r}) \cdot \vec{\nabla} \times \vec{L} h_L(\beta r) Y_{LM}(\vec{\Omega}) | \varphi_2 \rangle d\vec{r} \\ &\times \int \langle \psi_1 | \vec{j}_N(\vec{r}') \cdot \vec{\nabla} \times \vec{L} j_L(\beta r') Y_{LM}^*(\vec{\Omega}) | \psi_2 \rangle d\vec{r}' \end{aligned}$$

The long-wavelength limit yields the following expression for the nuclear part:

$$\begin{aligned} \int \langle \psi_1 | \vec{j}_N(\vec{r}) \cdot \vec{\nabla} \times \vec{L} j_L(\beta r) Y_{LM}^*(\vec{\Omega}) | \psi_2 \rangle d\vec{r} \\ = \frac{L+1}{(2L+1)!!} \omega_N \beta^L (-1)^{I_1 - M_2} \begin{pmatrix} I_1 & L & I_2 \\ -M_1 & -M & M_2 \end{pmatrix} \\ \times \langle I_1 || r^L Y_L || I_2 \rangle \end{aligned}$$

As for the electronic contribution it is calculated with solutions of Dirac's equation. Since the electronic orbits considered here are bound, an additional radial quantum number "n" is needed to specify the electron configuration  $|n\kappa m\rangle$ . The total angular momentum  $j$  is related to  $\kappa$  through the relation

$$j = |\kappa| - \frac{1}{2}.$$

Using the results in Ref. [2], one defines

$$\begin{aligned} \int \langle \varphi_1 | \vec{j}_e(\vec{r}) \cdot \vec{\nabla} \times \vec{L} h_L(\beta r) Y_{LM}(\vec{\Omega}) | \varphi_2 \rangle d\vec{r} \\ = \langle \kappa_1 m_1 | Y_{LM} | \kappa_2 m_2 \rangle \beta R_{n_1 \kappa_1 n_2 \kappa_2}(EL). \end{aligned}$$

The quantity  $R_{n_1 \kappa_1 n_2 \kappa_2}(EL)$  is a radial integral whose definition is given by formula (10.129) of Ref. [22]. One obtains finally the atom-nucleus coupling in the form

$$\begin{aligned} \langle \Psi_1 | R(E_{av} + i\epsilon) | \Psi_2 \rangle &= -i\sqrt{4\pi} \frac{\omega_N \beta^L}{L(2L+1)!!} \hat{L} \hat{j}_1 \hat{j}_2, \\ \sum_{L,M} (-1)^{I_1 - M_2 + m_1 + 1/2} \begin{pmatrix} I_1 & L & I_2 \\ -M_1 & -M & M_2 \end{pmatrix} \begin{pmatrix} j_1 & L & j_2 \\ \frac{1}{2} & 0 & -\frac{1}{2} \end{pmatrix} \\ &\times \begin{pmatrix} j_1 & L & j_2 \\ -m_1 & M & m_2 \end{pmatrix} \langle I_1 || r^L Y_L || I_2 \rangle R_{n_1 \kappa_1 n_2 \kappa_2} \end{aligned}$$

with the shorthand notation  $\hat{j} = \sqrt{2j+1}$ . Also, we have used the following expression for the electronic angular integral:

$$\begin{aligned} \langle \kappa_1 m_1 | Y_{LM} | \kappa_2 m_2 \rangle &= (-1)^{m_1 + 1/2} \frac{\hat{L} \hat{j}_1 \hat{j}_2}{\sqrt{4\pi}} \begin{pmatrix} j_1 & L & j_2 \\ \frac{1}{2} & 0 & -\frac{1}{2} \end{pmatrix} \\ &\times \begin{pmatrix} j_1 & L & j_2 \\ -m_1 & M & m_2 \end{pmatrix}. \end{aligned}$$

In order to calculate the probability of the NEET we also define the quantity  $R_{21}^2$  as

$$R_{21}^2 = \sum_{M_1, M_2, m_1, m_2} |\langle \Psi_1 | R(E_{av} + i\epsilon) | \Psi_2 \rangle|^2,$$

where the average is taken over the magnetic degeneracy of the initial and final configurations of the nucleus-atom system. This summation is readily expressed by means of the orthogonality relations satisfied by the  $3j$  coefficients. The result is

$$\begin{aligned} R_{21}^2 &= 4\pi\alpha \sum_L \frac{\omega_N^2 \beta^{2L}}{[L(2L+1)!!]^2} (2j_1+1)(2j_2+1) \\ &\times \begin{pmatrix} j_1 & L & j_2 \\ \frac{1}{2} & 0 & -\frac{1}{2} \end{pmatrix}^2 |R_{n_1 \kappa_1 n_2 \kappa_2}|^2 |\langle I_1 || r^L Y_L || I_2 \rangle|^2, \end{aligned}$$

where  $\alpha$  is the fine-structure constant and  $I_1, I_2$  are the angular momenta of the nuclear ground state and isomeric state, respectively. On the other hand  $j_1, j_2$  stand for the angular momenta of the electronic hole states. By introducing the usual definition

$$B(EL, I_2 \rightarrow I_1) = \frac{1}{2I_2+1} |\langle I_1 || r^L Y_L || I_2 \rangle|^2$$

from the formula above, one finally obtains the following expression:

$$\begin{aligned} R_{21}^2 &= 4\pi\alpha \sum_L \frac{\omega_N^2 \beta^{2L}}{[L(2L+1)!!]^2} (2j_1+1)(2j_2+1)(2I_2+1) \\ &\times \begin{pmatrix} j_1 & L & j_2 \\ \frac{1}{2} & 0 & -\frac{1}{2} \end{pmatrix}^2 |R_{n_1 \kappa_1 n_2 \kappa_2}|^2 B(EL, I_2 \rightarrow I_1). \end{aligned}$$

Note that in order to compare with other formulas given elsewhere one must use

$$B(EL, I_2 \rightarrow I_1) = \frac{2I_1+1}{2I_2+1} B(EL, I_1 \rightarrow I_2).$$

To our knowledge, when other authors have considered the NEET transition from an initial state  $[(I_1, M_1)(j_1, m_1)]$  they did not average as we did over the magnetic quantum number of the initial state. Consequently one must also divide the above expression by  $(2I_1+1)(2j_1+1)$  hence the result is

$$\begin{aligned} R_{21}^2 &= 4\pi\alpha \frac{\omega_N^{2L+2} \beta^{2L}}{[L(2L+1)!!]^2} \begin{pmatrix} j_1 & L & j_2 \\ \frac{1}{2} & 0 & -\frac{1}{2} \end{pmatrix}^2 |R_{n_1 \kappa_1 n_2 \kappa_2}|^2 \\ &\times B(EL, I_1 \rightarrow I_2). \end{aligned}$$

- [1] M. Morita, *Prog. Theor. Phys.* **49**, 1574 (1973).
- [2] E. V. Tkalya, *Nucl. Phys.* **A539**, 209 (1992).
- [3] S. Kishimoto *et al.*, *Phys. Rev. Lett.* **85**, 1831 (2000).
- [4] I. Ahmad *et al.*, *Phys. Rev. C* **61**, 051304 (2000).
- [5] K. Aoki *et al.*, *Phys. Rev. C* **64**, 044609 (2001).
- [6] M. Harston, *Nucl. Phys.* **A690**, 447 (2001).
- [7] R. Phillips *et al.*, *Phys. Rev. Lett.* **62**, 1025 (1989).
- [8] R. Phillips *et al.*, *Phys. Rev. A* **47**, 3682 (1993).
- [9] F. Attallah *et al.*, *Phys. Rev. Lett.* **75**, 1715 (1995).
- [10] F. Attallah *et al.*, *Phys. Rev. C* **55**, 1665 (1997).
- [11] T. Carreyre *et al.*, *Phys. Rev. C* **62**, 024311 (2000).
- [12] Y. Izawa *et al.*, *Phys. Lett.* **88B**, 59 (1979).
- [13] R. V. Arutyunyan *et al.*, *Yad. Fiz.* **53**, 36 (1991) [*Sov. J. Nucl. Phys.* **53**, 23 (1991)].
- [14] G. Malka *et al.*, *Proc. SPIE* **4510**, 58 (2001).
- [15] V. Méot *et al.* "Etude de l'excitation de l' $^{235}\text{U}$  dans un plasma: L'expérience ISOMERE sur PHEBUS," Rapport CEA-R-5944 (2000).
- [16] M. Harston and J. F. Chemin, *Phys. Rev. C* **59**, 2462 (1999).
- [17] R. W. P. McWhirter, in *Plasma Diagnostic Techniques*, edited by R. H. Huddlestone and S. L. Leonard (Academic, New York, 1965).
- [18] M. L. Goldberger and K. M. Watson, *Collision Theory* (Wiley, New York, 1964).
- [19] C. Cohen-Tannoudji, J. Dupont-Roc, and G. Grynberg, *Atom-Photon Interactions: Basic Processes and Applications* (Wiley, New York, 1998).
- [20] J. J. Niez, *C. R. Phys.* **3**, 1255 (2002).
- [21] J. J. Niez, *Phys. Rev. C* **67**, 024611 (2003).
- [22] H. C. Pauli, K. Alder, and R. M. Steffen, *The Electromagnetic Interaction in Nuclear Spectroscopy*, The Theory of Internal Conversion, Vol. 10 (North-Holland, Amsterdam, 1975).
- [23] B. F. Rozsnyai, *Phys. Rev. A* **5**, 1137 (1972).
- [24] I. M. Band and M. B. Trzhaskovskaya, *At. Data Nucl. Data Tables* **55**, 43 (1993).
- [25] M. Baranger, *Atomic and Molecular Processes*, edited by D. R. Bates (Academic Press, New York, 1962).
- [26] H. Nguyen *et al.*, *Phys. Rev. A* **33**, 1279 (1986).
- [27] M. Koenig *et al.*, *Phys. Rev. A* **38**, 2089 (1988).
- [28] L. Spitzer, Jr., *Physics of Fully Ionized Gases* (Wiley, New York, 1962).
- [29] G. Faussurier, C. Blancard, and A. Decoster, *J. Quant. Spectrosc. Radiat. Transf.* **58**, 571 (1997).
- [30] G. Faussurier, C. Blancard, and A. Decoster, *Phys. Rev. E* **56**, 3474 (1997).
- [31] G. Faussurier, C. Blancard, and A. Decoster, *Phys. Rev. E* **56**, 3488 (1997).
- [32] F. Perrot, *Physica A* **150**, 357 (1988).
- [33] S. J. Rose, *J. Phys. B* **25**, 1667 (1992).
- [34] D. W. Forslund *et al.*, *Phys. Rev. Lett.* **39**, 284 (1977).
- [35] K. Estabrook, *Phys. Rev. Lett.* **39**, 284 (1977).
- [36] G. Gosselin and P. Morel (unpublished).
- [37] M. Fajardo *et al.*, *Phys. Rev. Lett.* **86**, 1231 (2001).
- [38] D. Salzman, *Atomic Physics in Hot Plasmas* (University Press, Oxford, 1997).
- [39] H. R. Griem, *Phys. Rev.* **131**, 1170 (1963).
- [40] J. A. Bounds and P. Dyer, *Phys. Rev. C* **46**, 852 (1992).